# Single-Pulse Pulsed Laser Polymerization–Electron Paramagnetic Resonance Investigations into the Termination Kinetics of *n*-Butyl Acrylate Macromonomers

**Johannes Barth,[1] Michael Buback,[1] Christopher Barner-Kowollik,[2] Thomas Junkers,[3] Gregory T. Russell[4]**

[1]Institute for Physical Chemistry, University of Göttingen, Göttingen D-37077, Germany
[2]Preparative Macromolecular Chemistry, Institut für Technische Chemie und Polymerchemie, Karlsruhe Institute of Technology (KIT), Karlsruhe D-76128, Germany
[3]Polymer Reaction Design Group, Institute for Materials Research, Universiteit Hasselt, Agoralaan, Diepenbeek B-3590, Belgium
[4]Department of Chemistry, University of Canterbury, Christchurch, New Zealand
Correspondence to: G. T. Russell (E-mail: greg.russell@canterbury.ac.nz)

Received 2 May 2012; accepted 26 July 2012; published online 17 August 2012
**DOI: 10.1002/pola.26295**

**ABSTRACT**: The termination of model mid-chain radicals (MCRs), which mimic radicals that occur in acrylate polymerization over a broad range of reaction conditions, has been studied by single-pulse pulsed laser polymerization (SP-PLP) in conjunction with electron paramagnetic resonance spectroscopy. The model radicals were generated by initiator-fragment addition to acrylic macromonomers that were preformed prior to the kinetic experiments, thus enabling separation of termination from the propagation reaction, for these model radicals propagate sparingly, if at all, on the timescale of SP-PLP experiments. Termination rate coefficients of the MCRs were determined in the temperature range of 0–60°C in acetonitrile and butyl propionate solution as well as in bulk macromonomer over the range of 0–100 °C. Termination rate coefficients slightly below those of the corresponding secondary radicals were deduced, demonstrating the relatively high termination activity of this species, even when undergoing MCR–MCR termination. For chain length of 10, a reduction by a factor of 6 is observed. Unusually high activation energies were found for the termination rate coefficient in these systems, with 35 kJ mol$^{-1}$ being determined for bulk macromonomer. © 2012 Wiley Periodicals, Inc. J Polym Sci Part A: Polym Chem 50: 4740–4748, 2012

**KEYWORDS**: ESR/EPR; kinetics (polym.); macromonomers (acrylate); mid-chain radicals; radical polymerization; termination

**INTRODUCTION** Nowadays, it is undisputed that reaction steps associated with mid-chain radicals (MCRs) play an important role in both conventional and reversible-deactivation ("controlled/living") radical polymerization (RP) of acrylates.[1] Indeed, any study on acrylate RP that did not consider the role of MCRs would not be taken seriously. Yet, remarkably, it was only just over a decade ago that the occurrence of MCRs in RP of acrylates was first proven definitively: Ahmad et al. used $^{13}$C NMR to show the existence of branch points in poly(*n*-butyl acrylate),[2] and then a year later Chiefari et al. showed that high-temperature acrylate RP produces macromonomers (MMs) in high yield.[3] These studies may be taken as proof, explicit and implicit, respectively, of the occurrence of chain transfer to polymer in these systems.

Progress since this breakthrough has been swift, with long-standing conundrums being cleared up. For example, the strong nonclassical variation of rate of polymerization with monomer concentration, $c_{M,}$ that is observed in acrylates is now known to be a consequence of MCR formation followed by slow propagation[4]—in effect there is increasing self-retardation as $c_M$ becomes smaller. Similarly explained is the apparent variation of propagation rate coefficient, $k_{p,}$ with pulsing frequency in pulsed laser polymerization (PLP) experiments.[5]

These manifestations of MCR formation naturally elicit curiosity about how MCRs behave. Specifically, what reactions do they undergo and what values are taken by the rate coefficients for these reactions? Such information is essential for modeling the all-important quantities of rate of polymerization, molar mass distribution, and branching level. It is now well accepted that MCRs may potentially undergo all of termination, $\beta$-scission, addition—to monomer, to RAFT agent in RAFT polymerizations, and so on—and even halide transfer, for example in atom transfer radical polymerization (ATRP) systems.[1] However, while it is relatively easy to write down all these reactions, it has proven elusive to measure

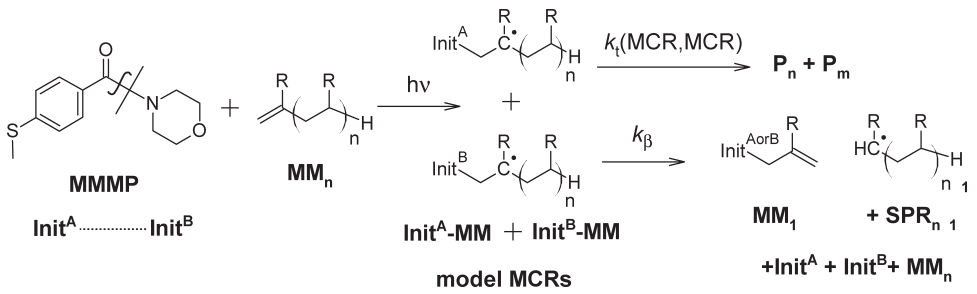


**SCHEME 1** Formation of model MCRs that can be used for studying MCR kinetics in the absence of SPRs. In this study, the fragments $Init^A$ and $Init^B$ arise from UV-induced decomposition of the photoinitiator MMMP. These then add to the MM (where *R* is *n*-Bu-*O*-CO- in this study) to form model MCRs, which react either by termination (most likely via disproportionation) or, at temperatures well above 80 °C, by $\beta$-scission. The latter reaction is just the reverse of the addition reaction that forms the model MCRs in the first place.

many of the associated rate coefficients. In the absence of such information, modeling becomes guesswork.

Especially for termination, there is this vexing situation of rate coefficients being difficult to measure. It is easy to explain why: the simultaneous presence of secondary propagating (chain end) radicals (SPRs) means that there are three different termination processes occurring at once, namely homotermination of SPRs, rate coefficient $k_t$(SPR, SPR), homotermination of MCRs, $k_t$(MCR, MCR), and crossterminationation between the two types of species, $k_t$(SPR, MCR). Originally it was hoped that the so-called SP-PLP–electron paramagnetic resonance (EPR) technique, which couples single-pulse (SP) PLP experiments with EPR spectroscopy,[6,7] might solve this problem, not just because it is the most powerful technique for studying termination kinetics,[8] but also by virtue of its ability to resolve the SPR and MCR populations and separately monitor their evolution with time.[9] However, this hope proved to be in vain, because it was found that the dominant impact of SPR–MCR crossterminationation renders MCR–MCR termination difficult to assess.[10] A similar problem arises with the $\beta$-scission (i.e., fragmentation) of MCRs, for which the significant contribution of MCR propagation prevents access to the much lower $\beta$-scission rate from SP-PLP–EPR data. Nevertheless, acrylate MCR fragmentation rates and activation energies, derived via other means, have been reported previously.[1]

In view of this situation, it appeals to circumvent these difficulties by finding a model system for the study of MCR termination kinetics in which interference by SPRs and by propagation does not occur. Such a system should be afforded by addition of primary radical fragments, denoted $Init^A$ and $Init^B$, from photoinitiator decomposition, to acrylate-type MMs: as is shown in Scheme 1, this generates tertiary radical species that are similar to the MCRs occurring during acrylate RP. The model MCRs, $Init^A$–MM· and $Init^B$–MM· (Scheme 1) should be able to crosspropagate in the presence of an acrylate,[11] just as conventional MCRs add to monomer in acrylate homopolymerizations. However, on account of the large steric hindrance, it is not expected that these model MCRs can add to MM on the timescale of an SP-PLP experiment. This has been confirmed by SEC and by mass spectrometric analysis of an MM reaction mixture before and after treatment with a thermal initiator up to complete decomposition: no observable increase in polymer size occurs.[12]

Such an observation is consistent with the measured $k_p$ for the so-called methyl acrylate[13] and butyl acrylate (BA)[14] dimers, which are about a factor of 1000 lower than $k_p$ for the corresponding acrylates. Specifically, for the BA dimer the average time that is required for a propagation step to take place is roughly 1 s at 20 °C (under the conditions of the present MM experiment in 10% solution assuming an average molar mass of 2000 g $mol^{-1}$). Thus, on the timescale of the experiments outlined herein, a little propagation would occur with the dimer. However, the BA dimer value may be considered as an upper bound for present purposes, as reduced propagation rates must be expected when increasing the size of the MM to chain length 3 or above. Hence, no significant propagation is expected in our experiments. Incidentally, the fact that steric hindrance is responsible for reduced propagation rate coefficients certainly engenders an expectation of reduced termination rate coefficients for MMs on account of the same cause.

As it so happens, acrylate MMs are readily obtainable as a result of recent intensive study;[15,16] indeed, Barner-Kowollik and Junkers prepared a library of such species.[17] Accordingly, in this study samples of *n*-BA MM will be examined via SP-PLP–EPR.[6] As just explained, the resulting radicals should be models for acrylate MCRs formed by backbiting (i.e., intramolecular chain transfer to polymer), and they should not readily propagate. Thus, to a good approximation, the decay in radical concentration, $c_R$, that is consequent upon a laser pulse should be given by

$$\frac{dc_R}{dt} = -2k_t(c_R)^2 \quad (1)$$

where the $k_t$ is for a termination process that mimics MCR homotermination. For this reason, the $k_t$ obtained from such SP-PLP–EPR experiments should be representative of $k_t$(MCR, MCR) values in acrylate RP. This, then, is what will be done in this article.

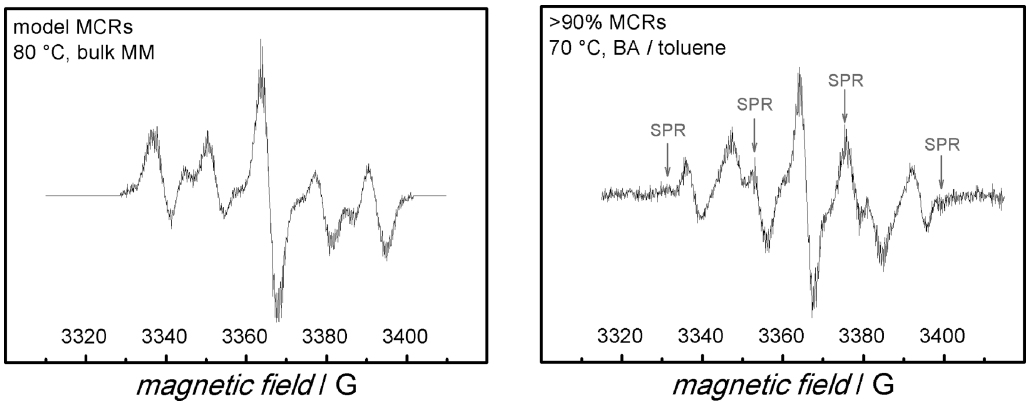


**FIGURE 1** Spectra recorded during continuous photoinitiation of MMMP in bulk MM (left-hand side; this study) and in BA solution (1.5 mol $L^{-1}$ in toluene; right-hand side[9]) at similar polymerization conditions and EPR settings. The low-intensity field positions associated with secondary propagating (chain end) radicals (SPRs) are indicated on the right-hand spectrum, making clear that the signal in the MM system is predominantly from MCRs.[9]

## EXPERIMENTAL

BA MM was synthesized as described elsewhere.[17] The solvents acetonitrile (AN; Sigma-Aldrich, 99.8%) and butyl propionate (BP; Aldrich, 99%) were used as received. Solutions of MM and solvent were degassed by several freeze–pump–thaw cycles. The photointiator α-methyl-4(methylmercapto)-α-morpholinopropiophenone (MMMP; Aldrich, 98%) was used as received. It was added to a solution in a glove box under an argon atmosphere to yield MMMP concentrations of $1.5 \times 10^{-2}$ mol $L^{-1}$. Sample volumes of 0.05 mL were filled into quartz tubes of 3 mm outer and 2 mm inner diameter.

The tubes were fitted into the EPR resonator cavity of a Bruker Elexsys E 500 series cw-EPR spectrometer. The samples were irradiated through a grid by a COMPex 102 excimer laser (Lambda Physik) operated on the XeF line (351 nm). The laser energy per pulse was around 80 mJ. The EPR spectrometer and the laser source were synchronized by a pulse generator (Scientific Instruments 9314). Temperature control was achieved via an ER 4131VT unit (Bruker) by purging the sample cavity with nitrogen. The decay in radical concentration after applying a single (laser) pulse at $t = 0$ was monitored via the EPR intensity at fixed magnetic field. To improve signal-to-noise quality, up to 10 individual $c_R(t)$ traces were coadded. EPR intensity was calibrated for absolute radical concentration via the procedure described elsewhere[6,18] that involves the stable radical compound 2,2,6,6-tetramethyl-1-piperidinyloxy (TEMPO; Aldrich, 99%), which was used without further purification. The entire experimental procedure has been described in greater detail in the previous study on SP-PLP–EPR.[6]

The SP-PLP–EPR experiments were carried out at temperatures between 0 and 100 °C for bulk MM and for MM dissolved in both BP and AN at MM weight fractions of between 10 and 85%.

## RESULTS AND DISCUSSION

### Demonstration of Concept

The EPR spectrum observed during continuous irradiation of a reaction mixture consisting of MM and MMMP is shown in Figure 1. As illustrated, the EPR signal for the model MCRs is found to be more or less identical to the spectrum recorded during an acrylate polymerization at 70 °C, where the fraction of MCRs is close to 90%.[9] This may be taken as proof of the idea behind this study, that is, that SP-PLP experiments involving MM as monomer will give information about MCR termination.

Having said that, there are some minor differences in the splitting patterns of the EPR spectra shown in Figure 1, that is, those from this study and from BA MCRs in the earlier study.[9] These arise from: (1) Restricted rotation around the carbon bond next to the radical functionality, which is more pronounced in the more viscous MM system,[9] and (2) small variation in coupling constants owing to the difference between the initiator fragments and an acrylate monomer unit.

### Data Analysis

For SP-PLP–EPR measurement on the MM/MMMP system, the intensity of the large, central EPR line of the MM signal—see the left-hand side of Figure 1—was monitored after applying an intense laser pulse. From this intensity, the radical concentration, $c_R$, was obtained as a function of time, $t$. These traces were fitted to eq 2, which follows from integration of the termination rate law, eq 1:[8,19]

$$\frac{c_R(t)}{c_R(0)} = (2k_t t\, c_R(0) + 1)^{-1} \qquad (2)$$

In this equation, $c_R(0)$ denotes the MCR concentration produced by addition of initiator fragments to MM directly after applying a laser SP at $t = 0$. This quantity is yielded by the EPR procedure. Hence, the only variable in the fitting is $k_t$, the value of which is thus delivered by this procedure. Equation 2 assumes there is no change of $k_t$ with time. If there is, then the fitting of eq 2 yields a time-averaged termination rate coefficient, $\langle k_t \rangle$. The fitting procedure is shown in Figure 2 for radical traces obtained with bulk MM at 0 and 80 °C.

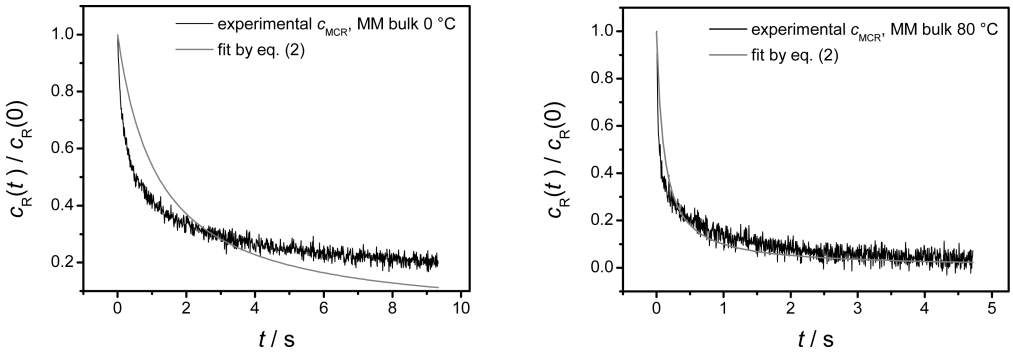


**FIGURE 2** MCR concentration, $c_R$, versus time, $t$, at 0 °C (left-hand side) and at 80 °C (right-hand side) from SP-PLP–EPR experiments with BA MM in bulk, where the initial MCR concentration, $c_R(0)$, has been determined by calibration. Traces: experimental data; curves: best fits of eq 2 to the data, yielding $k_t = 1.7 \times 10^4$ L mol$^{-1}$ s$^{-1}$ at 0 °C and $8.5 \times 10^5$ L mol$^{-1}$ s$^{-1}$ at 80 °C.

It should be no surprise from the above that the major source of experimental uncertainty in $k_t$ is error in $c_R(0)$.[6] As detailed elsewhere,[6,18] this has a number of causes, including concentration and filling level of TEMPO (used for calibration) and MM solutions; and mathematical processing of the experimental EPR spectra, viz. baseline adjustment and integration steps. The resulting error in $k_t$ is conservatively estimated to be 30%.[6,18,20] Note that there is also variation in $c_R(0)$ from experiment to experiment, even under ostensibly identical conditions.[6] This variation is typically 30–50%, and is a consequence of differences in laser light intensity and, at low temperatures, of condensation of water on the sample-tube surface. On top of this, there is variation of $c_R(0)$ owing to solvent amount. In our experiments, we at all times obtained physically realistic values of $c_R(0)$, and we found no correlation between scatter in $k_t$ values and variation of $c_R(0)$ values. This gives confidence that the error in our $k_t$ is random rather than systematic.

### Nonideality of Fits

The fits by eq 2, which are represented by the gray lines in Figure 2, deviate from the experimental $c_R(t)$ data in a systematic manner. Termination of model MCRs proceeds with higher rate coefficient at short times after applying the laser SP and with lower rate coefficient at longer $t$. This can be deduced from the fact that the best fits lie above the data at early times (i.e., the best-fit $k_t$ is too small) and below the data at late times. This is shown formally in Figure 3, which presents fits of eq 2 over discrete time intervals. Specifically, eq 2 is fitted where $c_R(t) > 0.35 \times c_R(0)$ and then separately for $c_R(t) < 0.35 \times c_R(0)$ (long times). It is found that $k_t$ from the early-time fitting is higher by a factor of 5 than $k_t$ from the long-time fitting, that is, there is a clear decrease of $k_t$ during the course of an SP-PLP. A number of suggestions occur for explaining this situation; four of these—by no means an exhaustive list—will now be discussed in turn.

1. *Chain-length-dependent termination owing to radical growth*. The termination rate coefficient of the model MCRs appears to decrease with time after pulsing. Such a decrease in $k_t$ has been observed in all SP-PLP–EPR results to date,[6,20,21] and has been uncontroversially assigned to chain-length-dependent termination (CLDT):[6,22] as the radicals grow during the time period of the experiment, $k_t$ declines. However, this explanation is highly unlikely to be applicable for MMs, which are expected to propagate too slowly[13,14] on the timescale of SP-PLP–EPR measurements for any significant growth in chain length to occur.[12] That said, the door should not be fully closed on this suggestion until it has been specifically investigated.
2. *Temperature*. Inspection of the $c_R(t)$ traces in Figure 2 seems to indicate that increasing temperature allows for better fitting with eq 2, that is, a single $k_t$ value becomes more appropriate as temperature is raised, and thus one should search for an explanation for nonideality that is related to temperature. However, Figure 4 shows that such thinking is spurious: it is shown that when the data of Figure 2 are replotted so that the timescales are kinetically equivalent, the deviations from ideality are more-or-less the same. In other words, the impression from Figure 2 that the 80 °C data are better described by eq 2 is an optical illusion created by the much lower relative radical

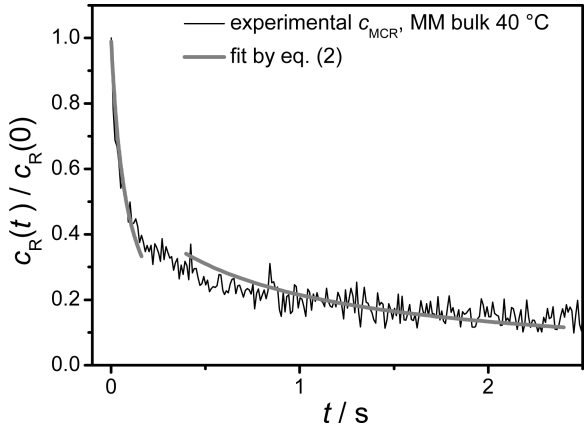


**FIGURE 3** As for Figure 2, but with data from 40°C, and carrying out separate fitting for shorter and for longer times (see text), where the division between the two regions has been (arbitrarily) set at 35% of the initial radical concentration. The early-time fit yields $k_t$ that is half an order of magnitude larger than $k_t$ from the late-time fit.

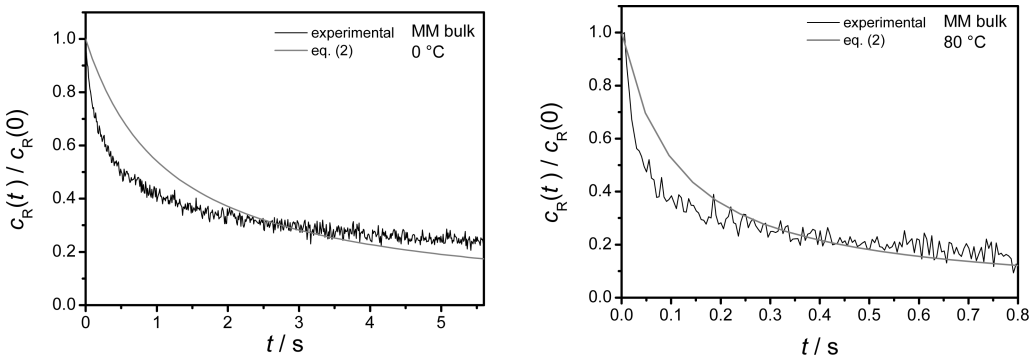


**FIGURE 4** As for Figure 2, but presenting the data so that each intersection of the experimental data and the best fit of eq 2 is located at the mid-point of the time axis.

concentration that is reached, owing to the higher $k_t$, on the timescale of the experiment. In view of this, it may be said that the results are nonideal at all temperatures, and that deviations from ideality are not owing to a side reaction that becomes less influential at higher temperature.

3. *CLDT owing to MM polydispersity*. As shown in Figure 5, the utilized MM sample is polydisperse: it is known[15,17] that BA MMs with degree of polymerization between 3 and about 50 are contained in the initial MM sample of average chain length about 10. Kinetic simulations have shown that such polydispersity is an unavoidable consequence of the formation chemistry.[23] Making the reasonable assumption that MMs of all sizes react with the MMMP fragments $Init^A$ and $Init^B$ (Scheme 1) at a rate that is fast on the timescale of termination, our SP-PLP–EPR experiments, therefore, must have had a chain-length distribution of radicals at $t = 0$ that mirrors the size distribution of the initial MM mixture as shown in Figure 5. Given that this distribution is polydisperse and that there is no obvious reason why MM radicals should not display CLDT termination, one therefore must expect that our MM sample was characterized by a spectrum of termination rate coefficients, which is contrary to what eq 2 assumes. Note that this situation may sound similar to that of standard monomers with SP-PLP–EPR, but in fact it is different: in the usual situation there is decrease of $k_t$ with $t$ as the (relatively) monodisperse radical population propagates to become longer in size, whereas in the present case there are different but fixed radical sizes present at all times. Thus, the equations used to account for CLDT in SP-PLP–EPR experiments[24] are not applicable.

Given this, we conducted simulations with the PREDICI® software package[25] to investigate the effect of radical polydispersity on SP-PLP–EPR kinetics. The input distribution of radical sizes was the measured one of Figure 5. The total initial MCR concentration was set to $c_R(0) = 1 \times 10^{-5}$ mol $L^{-1}$, a typical order of magnitude for this quantity. The so-called composite model for termination[26] was employed:

$$\begin{aligned} k_t^{i,i} &= k_t^{1,1} i^{-\alpha_s}, \quad i \le i_c \\ k_t^{i,i} &= k_t^{1,1} (i_c)^{-\alpha_s+\alpha_1} i^{-\alpha_1} \equiv k_t^0 i^{-\alpha_1}, \quad i > i_c \end{aligned} \tag{3}$$

Equation 3 has been found to describe CLDT in essentially all systems investigated to date.[6,22] BA literature values[10,20] of the long-chain exponent, $\alpha_l$, and the crossover chain length, $i_c$, were adopted here. Note that these values are of very low importance, as the average degree of polymerization of the MM sample under investigation is about 10 (Fig. 5), which is well below the average acrylate value for $i_c$ of 30.[20] This means that the vast majority of termination events involve "small" radicals, and hence the parameters $\alpha_s$, the so-called small-chain exponent, and $k_t^{1,1}$, the rate coefficient for termination between two species with $i = 1$, are crucial. For chain-end radicals in acrylate polymerization, an average value of $\alpha_s = 0.79$ has been found.[20] For acrylate MCRs, this value may be different; on the basis of long-chain studies one might expect it to be slightly higher for radical functionality a little removed from the chain end.[27] However, the value should not exceed unity.[21] Therefore, we decided to use $\alpha_s = 1$, as this should give maximum possible effect for the idea under consideration, and hence indicate whether it

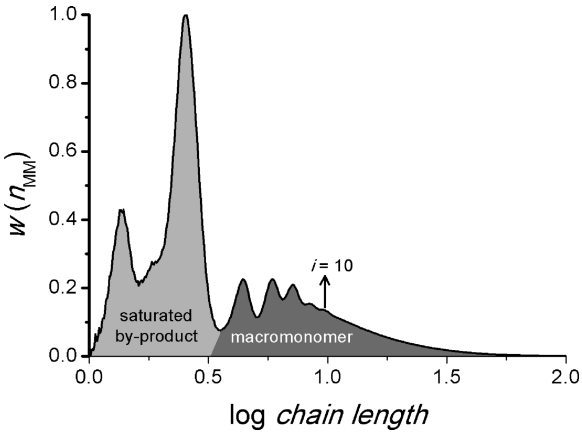


**FIGURE 5** Chain-length distribution of the BA MM sample[15,17] used for the SP-PLP–EPR studies of this study. The chain-length distribution was obtained as part of this study by size-exclusion chromatography with the calibration referring to poly(styrene) standards. The fraction of saturated by-product from MM synthesis, shown as a light gray area, is that after reduction by distillation, done as part of this study.

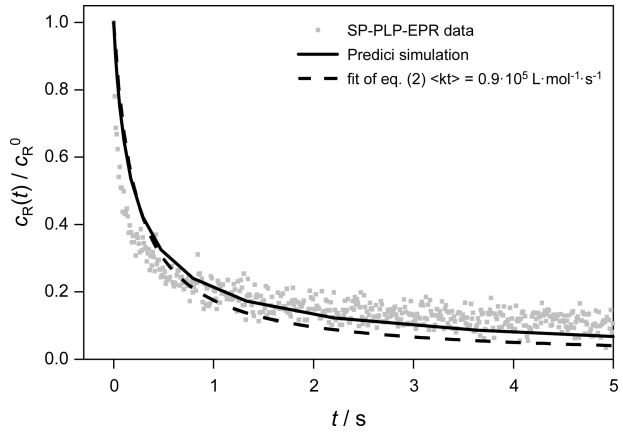


**FIGURE 6** SP-PLP–EPR experimental results for bulk MM at 40 °C (points) (see Fig. 2 for other temperatures but otherwise analogous conditions). The dashed line represents the best fit of the data to eq 2, whereas the full line is the improved match from a simulation taking CLDT into account with model and parameter values as detailed in the text.

is at all a possible explanation for the nonideality of our $c_R(t)$ traces. (Note that by now CLDT is considered to be normal;[6,22] the term "nonideal" should be interpreted to mean "not fitted by eq 2," rather than that there is anything unusual about CLDT.)

Simulation results are shown in Figure 6. The geometric-mean model was employed for crosstermination:

$$k_t^{i,j} = (k_t^{i,i} k_t^{j,j})^{0.5} \quad (4)$$

The value $k_t^{1,1} = 1 \times 10^6$ L mol$^{-1}$ s$^{-1}$ was chosen as it was found to give a good match between simulation output and measured signal trace for bulk MM at 40 °C, as is evident from Figure 6. Figure 6 shows that while the best fit of the data to eq 2 (dashed line) has the above-described deviation from ideality, an improved match is obtained with the simulation data (full line); in fact, radical concentrations at longer delay times are very well reproduced. At short times after the laser pulse, a somewhat faster decay in radical concentration is still observed in the experiment compared with the simulation. Despite the fact that a slightly higher starting radical concentration was assumed for simulation compared with the experimental trace, the simulation gives a good qualitative indication that chain-length dependence contributes to the identified nonidealities.

In physical terms, what is happening here? Because of the faster termination of small radicals, the chain-length distribution of the model MCRs varies with time after applying the laser pulse at $t = 0$. Specifically, there is a gradual shift in MM size distribution toward longer chain lengths, as the smaller radicals preferentially terminate, and this shift causes $\langle k_t \rangle$, the average over all chain lengths, to decrease as time proceeds.

Incidentally, note that the best-fit $k_t$ for the simulation results is extremely close in value to $k_t^{1,1} \times DP_n^{-\alpha_s}$ (cf. eq 3), where $DP_n \approx 10$ is the number-average degree of polymerization of the MM sample (see above). Such an outcome should not come as a surprise to those familiar with the theory of CLDT,[22] and is a useful result that will shortly be exploited.

4. *Kinetically distinct macroradicals from photoinitiation*. The photoinitiator MMMP dissociates into two structurally different fragments and hence, in principle, two chemically distinct species are available for the termination in this study, viz. Init$^A$–MM· and Init$^B$–MM· (Scheme 1). It is conceivable that these two species could have quite different termination reactivity, because the pendant group can markedly influence $k_t$ via steric effects.[6,22] For example, highly hindered monomers such as BA dimer,[14] di-*n*-butyl itaconate,[28] and dimethyl itaconate[29] have been found to have $k_t$ about one to two orders of magnitude lower than equivalent monomers without such steric hindrance.[14] If such an effect is occurring with Init$^A$–MM· and Init$^B$–MM·, then it may give rise to nonideality in $c_R(t)$ traces.

To investigate this idea, further simulations with PREDICI® were carried out. Figure 7 shows results from using $k_t$(A, A) $= 1 \times 10^5$ L mol$^{-1}$ s$^{-1}$, $k_t$(A, B) $= 1 \times 10^4$ L mol$^{-1}$ s$^{-1}$, and $k_t$(B, B) $= 5 \times 10^3$ L mol$^{-1}$ s$^{-1}$, where A and B denote Init$^A$–MM· and Init$^B$–MM·, respectively. As earlier with $k_t$(SPR, SPR), etc., a different notation to $k_t^{i,j}$ is used so as to convey that the variation here in individual $k_t$ is not owing to chain length. In effect, this model is just a simplified version of CLDT, where now there are only two states ("A" and "B") rather than all possible chain lengths, and both states start off with equal population, as opposed to the complicated starting distribution of Figure 5. Having initially equal concentrations of A and B species assumes that both photoinitiator fragments add equally well to MM and that no persistent (initiator derived) radical is present.

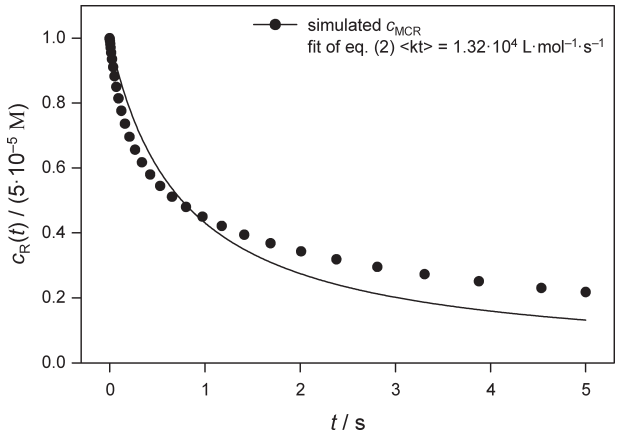


**FIGURE 7** Points: values of MCR concentration, $c_R$, as a function of time, $t$, from an SP-PLP simulation with $k_t$(A, A) $= 1 \times 10^5$ L mol$^{-1}$ s$^{-1}$, $k_t$(A, B) $= 1 \times 10^4$ L mol$^{-1}$ s$^{-1}$ and $k_t$(B, B) $= 5 \times 10^3$ L mol$^{-1}$ s$^{-1}$ in a two-state model (see text) with $c_R(0) = 5 \times 10^{-5}$ mol L$^{-1}$. Curve: best fit of eq 2 to the simulation results, yielding $k_t$ of intermediate value, as indicated.

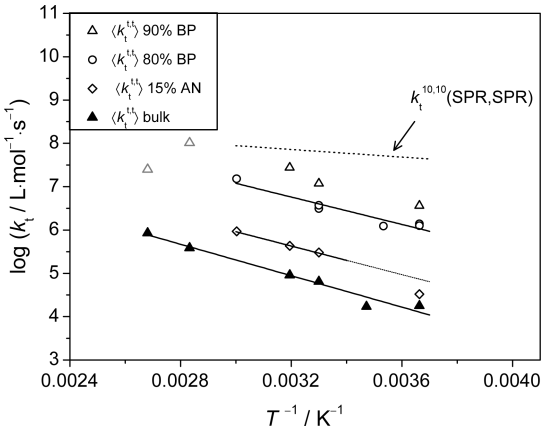


**FIGURE 8** Arrhenius plot of all $k_t$(MCR, MCR) values from fitting of eq 2 to SP-PLP–EPR experiments of this study, where $T$ is absolute temperature. Points: values for (bottom to top) BA MM in bulk (filled triangles), in 15 wt % AN (open diamonds), 80 wt % BP (open circles), and 90 wt % BP (open triangles). Lines: Arrhenius fits to the data sets (with the exception of the data for 10 wt % MM; see Table 1 for resulting parameter values), as well as (top line) low-conversion BA values of $k_t^{10,10}$(SPR, SPR) (i.e., homotermination of SPR 10-mers), as obtained in the previous SP-PLP–EPR studies.[10,20]

Of course, the given values of $k_t$(A, A), $k_t$(A, B), and $k_t$(B, B), while plausible, are nevertheless somewhat arbitrary, as they must be in the absence of hard-and-fast data. With different values for these parameters, one can obtain varying degrees of nonideality in $c_R(t)$ traces. The results shown in Figure 7 are simply those from a set of not unreasonable $k_t$ values that yield $c_R(t)$ qualitatively similar to our experimental data. That the latter is the case can be seen by comparing Figure 7 with earlier figures in which fits of eq 2 to experimental data are presented: the deviations are of the same magnitude and nature. This shows that the present model is capable of explaining the experimental data. This would be even more so the case where further chemical subtleties to be incorporated into modeling, for example that Init$^A$–MM· and Init$^B$–MM· may form on different timescales as a result of the photoinitiator fragments Init$^A$ and Init$^B$ adding to MM at significantly different rates, or that Init$^A$ and Init$^B$ may have different rates of self-termination, which will also give rise to disparate concentrations of Init$^A$–MM· and Init$^B$–MM·—clearly there are many possibilities for further investigation if desired.

It is also important to note about the simulation results of Figure 7 that when fitted by eq 2, they yield an overall $k_t$ that is representative of the input termination rate coefficients.

*Summation*. Two plausible models have been found for qualitatively explaining the nonideality in our $c_R(t)$ traces; indeed, it is quite possible that both effects may play a role in reality. Certainly, the CLDT explanation should be operative, because it is based on well-established facts, namely that the starting MM distribution is polydisperse and that termination is chain-length dependent. However, the investigative simulation of this study adopted what is considered to be the strongest possible extent of CDLT (viz. $\alpha_s = 1$), and yet the resulting deviation from ideality may not be as strong as that observed in experiments (Fig. 6). Hence, it may be that markedly different termination rate coefficients for Init$^A$–MM· and Init$^B$–MM·—most likely as a result of steric effects—are an extra cause of nonideality in $c_R(t)$ to a significant extent. There is much scope, through altered parameter values and extra mechanistic subtleties (some of which have been mentioned), for obtaining better quantitative agreement with the data. Our main intention here has just been to show qualitatively that this is possible, which we believe we have done.

Be all this as it may, the most important point here is that although eq 2 does not perfectly fit our experimental $c_R(t)$ traces, it has been established that these nonidealities may be explained within a conventional termination framework, and that the $k_t$ values obtained from fitting eq 2 are still representative of the termination processes occurring. Thus, one may be confident that the MM system under investigation is well suited for studying MCR kinetics via SP-PLP–EPR.

## RESULTS

Arrhenius plots of $k_t$ values of this study—as procured from best fitting of eq 2 to SP-PLP–EPR data—are shown in Figure 8. Values of Arrhenius parameters are listed in Table 1, as obtained from (straight line) Arrhenius fits. For bulk MM and for the most dilute MM solution (10 wt % in BP), temperature was varied between 0 and 100 °C. No Arrhenius fit is given for 10 wt % MM in BP, as the scatter in the measured data, in particular at higher temperature, is significant. For the two intermediate dilutions of MM, the temperature range was 0–60 °C, and hence fewer data points were obtained; further, in the case of the MM mixture containing 15 wt % AN, an outlier point was omitted from Arrhenius fitting (see Table 1). BP was used as a solvent because it is the saturated analogue of BA, the significance of which will be shortly seen; AN was employed because it is a common (co)solvent in ATRP of acrylates, and hence the resulting $k_t$ values may be of interest for ATRP modeling.

**TABLE 1** Activation Energy, $E_a$, and Pre-Exponential Factor, $A$, for $k_t$(MCR, MCR) Values of This Study, as Obtained from Arrhenius Fits of Figure 8

| System[a] | $E_a$ (kJ mol$^{-1}$) | $A$ (L mol$^{-1}$ s$^{-1}$) | Temperature Range[b] |
|---|---|---|---|
| Bulk MM | 35 ± 5 | $5.6 \times 10^{10}$ | 0–100 °C |
| 85 wt % MM in AN | 32 ± 7 | $8.1 \times 10^{10}$ | 0–60 °C[c] |
| 20 wt % MM in BP | 30 ± 5 | $6.6 \times 10^{11}$ | 0–60 °C |

[a] MM, macromonomer; AN, acetonitrile; and BP, butyl propionate.
[b] Range of temperatures for which $k_t$ was measured (Fig. 8), and therefore for which the given Arrhenius parameters hold.
[c] 0°C point omitted from Arrhenius fit, as deemed an outlier (inspect Fig. 8).

## DISCUSSION OF RESULTS

First, there is no evident curvature in the Arrhenius plots of Figure 8. If a side reaction such as $\beta$-scission, which has a relatively high activation energy, was coming into play at higher temperature, then the resulting SPRs would be expected to terminate more quickly than MCRs, thereby giving rise to a higher system $k_t$, and thus to non-Arrhenius behavior in log $k_t$ versus $T^{-1}$. The fact that this is not observed gives confidence that the measured decay of $c_R$ with $t$ is entirely (or at least largely) owing to MCR termination under all conditions.

Next, we consider the activation energies of Table 1. These $E_a$ values are unusually high. In the previous SP-PLP–EPR study, it has consistently been found that the measured $E_a(k_t^{1,1})$ is equal, within experimental error, to the measured $E_a(\eta^{-1})$, where $\eta$ denotes the viscosity of the monomer–solvent system.[6,20,21] This is as expected for a diffusion-controlled reaction between small molecules. Unfortunately, $\eta$ as a function of temperature, and hence $E_a(\eta^{-1})$, is not available for the bulk MM and MM/solvent systems of this study. However, what may be said is that the MM samples used in this study are highly viscous by small-molecule norms, exactly as one would expect of MM (which, after all, is small polymer). Thus, it cannot be excluded that $E_a(\eta^{-1})$ may approach values as high as the $E_a(k_t)$ measured here for bulk MM. Furthermore, one notes that our $E_a(k_t)$ seems to decline toward more normal small-molecule values of $E_a(\eta^{-1})$ as solvent is added, which is as one would expect for diffusion control, although one cannot be sure that this trend is really present in the data, because the variation of $E_a$ is within the limits of experimental uncertainty (Table 1). In fact, the closeness of the $E_a(k_t)$ for bulk MM and for 20 wt % MM in BP suggests that reduced segmental mobility owing to steric hindrance is the more likely explanation for the $E_a(k_t)$ being as high as they are. Large activation energies, for example, of about $E_a(k_t^{1,1}) = 28$ kJ mol$^{-1}$, have already been measured for di-*n*-butyl itaconate and assigned to the impact of steric shielding[14,28] (although admittedly this was also in the absence of any information on solvent viscosity).

Considering now the values of $k_t$, we first of all note that the relative ordering is as one would expect on the basis of diffusion control: as $\eta$ decreases in changing from 100% (bulk) MM to 85% MM to 20% MM to 10% MM, $k_t$ increases (Fig. 8). At 30 °C, for example, this increase in $k_t$ amounts to more than two orders of magnitude.

In terms of absolute values, there are two comparisons we may make, both relating to our system of 10 wt % MM in BP. This solvent was chosen because, as already mentioned, it is the saturated analogue of *n*-BA, and hence in physical terms it should mimic MM being surrounded by the analogous monomer. Thus, it is reasonable to compare this data set with the values from bulk BA polymerization.

The first comparison is with bulk BA values of $k_t^{10,10}$(SPR, SPR) (i.e., homotermination of SPR 10-mers) at low conversion, as obtained in the previous SP-PLP–EPR studies.[10,20] This is the top line in Figure 8. The reason for choosing chain length 10 is that, as mentioned earlier, our derived $k_t$ probably correspond reasonably closely to $k_t^{10,10}$(MCR, MCR) values. At 30 °C, our $k_t$(MCR, MCR) value for 10 wt % MM in BP is about a factor of 6 lower than $k_t^{10,10}$(SPR, SPR) for BA (Fig. 8). Some of this difference can be assigned to higher viscosity owing to the 10 wt % MM. However, it is highly unlikely that $\eta$ changes can nearly explain the full extent of the difference. Thus, these results suggest more steric shielding and reduced segmental mobility of the model MCRs in comparison with SPRs. This should not come as a surprise, because it is commonly accepted that MCRs have significantly lower $k_t$ than equivalent SPRs;[4] indeed, if anything the surprise might be that the effect only seems to amount to about a factor of 5.

The second comparison is with chain-length-averaged $k_t$(MCR, MCR) from steady-state BA bulk polymerization. From carrying out detailed data analysis,[30] Nikitin and Hutchinson have estimated for this quantity:[31]

$$k_t(\text{MCR, MCR}) = 1.8 \times 10^7 \text{ L mol}^{-1} \text{ s}^{-1} \exp[-5.6 \text{ kJ mol}^{-1}/(RT)] \quad (5)$$

Equation 5 gives $k_t = 2.0 \times 10^6$ L mol$^{-1}$ s$^{-1}$ for 30 °C, as compared with $k_t = 1.4 \times 10^7$ L mol$^{-1}$ s$^{-1}$ at 30 °C from using the Arrhenius parameters for 10 wt % MM in BP. This is a difference of a factor of 7, which most logically is owing to CLDT: MCR chain lengths are much larger in steady-state BA polymerization than in this study (Fig. 5), resulting in lower $k_t$ than found here.

Incidentally, the $E_a$ of eq 5 is noticeably lower than those of Table 1. In this context, it is interesting that the most recent modeling study by Nikitin et al. recommends the quite different values of $A = 5.3 \times 10^9$ L mol$^{-1}$ s$^{-1}$ and $E_a = 19.6$ kJ mol$^{-1}$ for (chain-length averaged) $k_t$(MCR, MCR) in steady-state BA solution polymerization.[32] These values are more in line with those of this study (Table 1), but they still give essentially the same value as eq 5 for 30 °C ($2.2 \times 10^6$ L mol$^{-1}$ s$^{-1}$), meaning that the argumentation above is unaffected.

From the two comparisons given here, it may be said that $k_t$(MCR, MCR) from this study is perfectly consistent with the values from similar but slightly different literature systems. This instills yet more confidence in the values from the present investigation.

Finally, we would like to stress that the Arrhenius fits of Figure 8 should not be used outside the temperature range of measurement; doing so may among other things lead to unjustified mechanistic conclusions.

## CONCLUSION

Investigations into termination are rarely straightforward; invariably there are difficulties in explaining all aspects of the data.[22] In this respect, this study is no exception, for example there has been the nonsimple nature of $c_R(t)$ traces (in the sense that they are not adequately fit by eq 2) and the uncommonly high values of $E_a(k_t)$. Nevertheless,

plausible explanations for these and all other features of our data have been found. What may not be noticed owing to all this commotion is a simple but very important finding: how *normal* are the $k_t$ values we have found for our model chain-end MCR radicals. What we mean by this is how well they nestle in with the literature values for BA systems and how comfortably they sit with the current knowledge about termination. Certainly, acrylate-derived MCRs seem to have $k_t$ values that are slightly lower than analogous SPRs, which is as one would expect. However, the values are not uncommonly lower, and our MCRs show a typical kind of termination kinetics[22] without any anomalies.

In terms of future study, several doors have been opened. Most obviously, it would be useful to measure MM viscosities, to carry out SP-PLP–EPR experiments with monodisperse MM samples, and to use a photoinitiator that results in MCR species of essentially equal termination reactivity (as opposed to the speculation here that $Init^A$–MM· and $Init^B$–MM· have significantly different $k_t$). More adventurously, the present MM system might be used for estimates of MCR $\beta$-scission (i.e., fragmentation) rates at higher temperature. These experiments should preferably be carried out under conditions of low termination rate, that is, in solution of a highly viscous compound such as naphthalin.

## ACKNOWLEDGMENTS

J. B. is grateful to the *Fonds der Chemischen Industrie* for a doctoral fellowship. G. T. R. thanks the University of Canterbury for provision of study leave, during which this project was carried out. C. B.-K. acknowledges continued support from the Karlsruhe Institute of Technology (KIT) in the context of the *Excellence Initiative* for leading German universities. T. J. is grateful for funding from the *Fonds Wetenschappelijk Onderzoek (FWO)* in the framework of the Odysseus scheme. The authors are grateful to Anna-Marie Zorn (KIT) for the provision of the MM and to Joachim Morick (UoG) for support with some of the experiments.

## REFERENCES AND NOTES

**1** Junkers, T.; Barner-Kowollik, C. *J. Polym. Sci. Part A: Polym. Chem.* **2008,** *46*, 7585–7605.

**2** Ahmad, N. M.; Heatley, F.; Lovell, P. A. *Macromolecules* **1998,** *31*, 2822–2827.

**3** Chiefari, J.; Jeffery, J.; Mayadunne, R. T. A.; Moad, G.; Rizzardo, E.; Thang, S. H. *Macromolecules* **1999,** *32*, 7700–7702.

**4** Nikitin, A. N.; Hutchinson, R. A. *Macromolecules* **2005,** *38*, 1581–1590.

**5** Nikitin, A. N.; Castignolles, P.; Charleux, B.; Vairon, J. P. *Macromol. Rapid Commun.* **2003,** *24*, 778–782.

**6** Barth, J.; Buback, M. *Macromol. React. Eng.* **2010,** *4*, 288–301.

**7** Buback, M.; Egorov, M.; Junkers, T.; Panchenko, E. *Macromol. Rapid Commun.* **2004,** *25*, 1004–1009.

**8** Barner-Kowollik, C.; Buback, M.; Egorov, M.; Fukuda, T.; Goto, A.; Olaj, O. F.; Russell, G. T.; Vana, P.; Yamada, B.; Zetterlund, P. B. *Prog. Polym. Sci.* **2005,** *30*, 605–643.

**9** Barth, J.; Buback, M.; Hesse, P.; Sergeeva, T. *Macromol. Rapid Commun.* **2009,** *30*, 1969–1974.

**10** Barth, J.; Buback, M.; Hesse, P.; Sergeeva, T. *Macromolecules* **2010,** *43*, 4023–4031.

**11** Zorn, A.-M.; Junkers, T.; Barner-Kowollik, C. *Macromolecules* **2011,** *44*, 6691–6700.

**12** Junkers, T., unpublished work.

**13** Tanaka, K.; Yamada, B.; Fellows, C. M.; Gilbert, R. G.; Davis, T. P.; Yee, L. H.; Smith, G. B.; Rees, M. T. L.; Russell, G. T. *J. Polym. Sci. Part A: Polym. Chem.* **2001,** *39*, 3902–3915.

**14** Buback, M.; Junkers, T.; Müller, M. *Polymer* **2009,** *50*, 3111–3118.

**15** Junkers, T.; Bennet, F.; Koo, S. P. S.; Barner-Kowollik, C. *J. Polym. Sci. Part A: Polym. Chem.* **2008,** *46*, 3433–3437.

**16** Koo, S. P. S.; Junkers, T.; Barner-Kowollik, C. *Macromolecules* **2009,** *42*, 62–69.

**17** Zorn, A. M.; Junkers, T.; Barner-Kowollik, C. *Macromol. Rapid Commun.* **2009,** *30*, 2028–2035.

**18** Barth, J.; Buback, M.; Hesse, P.; Sergeeva, T. *Macromolecules* **2009,** *42*, 481–488.

**19** Buback, M.; Hippler, H.; Schweer, J.; Vogele, H. P. *Makromol. Chem. Rapid Commun.* **1986,** *7*, 261–265.

**20** Barth, J.; Buback, M.; Russell, G. T.; Smolne, S. *Macromol. Chem. Phys.* **2011,** *212*, 1366–1378.

**21** Barth, J.; Siegmann, R.; Beuermann, S.; Russell, G. T.; Buback, M. *Macromol. Chem. Phys.* **2012,** *213*, 19–28.

**22** Barner-Kowollik, C.; Russell, G. T. *Prog. Polym. Sci.* **2009,** *34*, 1211–1259.

**23** Junkers, T.; Barner-Kowollik, C. *Macromol. Theory Simul.* **2010,** *18*, 421–433.

**24** Smith, G. B.; Russell, G. T. Z. *Phys. Chem. (Munich)* **2005,** *219*, 295–323.

**25** Wulkow, M. *Macromol. Theory Simul.* **1996,** *5*, 393–416.

**26** Smith, G. B.; Russell, G. T.; Heuts, J. P. A. *Macromol. Theory Simul.* **2003,** *12*, 299–314.

**27** Fröhlich, M. G.; Vana, P.; Zifferer, G. *J. Chem. Phys.* **2007,** *127*, 164906.

**28** Buback, M.; Egorov, M.; Junkers, T.; Panchenko, E. *Macromol. Chem. Phys.* **2005,** *206*, 333–341.

**29** Vana, P.; Yee, L. H.; Barner-Kowollik, C.; Heuts, J. P. A.; Davis, T. P. *Macromolecules* **2002,** *35*, 1651–1657.

**30** Nikitin, A. N.; Hutchinson, R. A. *Macromol. Theory Simul.* **2006,** *15*, 128–136.

**31** Nikitin, A. N.; Hutchinson, R. A. *Macromol. Rapid Commun.* **2009,** *30*, 1981–1988.

**32** Nikitin, A. N.; Hutchinson, R. A.; Wang, W.; Kalfas, G. A.; Richards, J. R.; Bruni, C. *Macromol. React. Eng.* **2010,** *4*, 691–706.